Reactions of Vanadium Oxide Cluster Ions with 1,3-Butadiene and Isomers of Butene†

R. C. Bell and A. W. Castleman, Jr.*

Department of Chemistry, The Pennsylvania State University, University Park, Pennsylvania 16802

Received: February 27, 2002

The gas-phase reactions of vanadium oxide cluster ions with 1,3-butadiene and the isomers of butene are examined. The correlation between the reaction products and the cluster stoichiometry, oxidation and charge-state are explored by studying the reactivity of 1,3-butadiene (C_4H_6) and the deuterated 1,3-butadienes C_4D_6 and 1,1,4,4-$C_4D_4H_2$ with the clusters cations $V_3O_6^+$, $V_3O_7^+$, and $V_3O_8^+$ and the anions $VO_{2,3}^-$, $V_2O_{4-6}^-$, $V_3O_{6-9}^-$ and $V_4O_{10,11}^-$. These studies further our understanding of the reactions of $V_xO_y^+$ clusters with hydrocarbons, as reported previously [Bell, R. C.; Zemski, K. A.; Kerns, K. P.; Deng, H. T.; Castleman, Jr., A. W. *J. Phys. Chem. A* **1998**, *102*, 1733], by examining the reaction of the anions ($V_xO_y^-$), deuterated butadiene species and the 2-butenes. The reactions of C_4D_6 and 1,1,4,4-$C_4D_4H_2$ with the cluster $V_3O_7^+$ demonstrate pathways for the loss of a single oxygen, oxidative dehydrogenation, and molecular association, as well as other minor products, analogous to the products previously reported for the reactions of these clusters with C_4H_6. The reactions of $V_3O_7^+$ with the isomers of butene (1-butene, *cis*-2-butene and *trans*-2-butene) display many of the same reaction pathways that are observed for 1,3-butadiene, namely, oxidation of the hydrocarbon, oxidative dehydrogenation, and molecular association. In addition, a major channel representing the dehydrogenation of the alkene and a minor channel for C2−C3 cracking of the alkene, along with other minor products is also observed. The anionic clusters $VO_{2,3}^-$, $V_2O_{4,5}^-$, $V_3O_{6-8}^-$, and $V_4O_{10}^-$ do not react with either 1,3-butadiene or 1-butene, whereas clusters of higher oxygen content, $V_2O_6^-$, $V_3O_9^-$, and $V_4O_{11}^-$ display a minor reaction channel for the loss of a single oxygen atom, presumably through oxidation of the hydrocarbon and resulting in the cluster $V_xO_{y-1}^-$.

Introduction

Transition metals and their oxides have been used for more than a century to manipulate chemical reactions. Their ubiquitous presence is due to the ability of these metals to adopt different oxidation states, stoichiometries, and coordination modes. However, this enormous diversity represents a challenge to chemists in their attempt to identify, understand, and finally, predict reaction mechanisms. Catalytic oxidation by such materials generally proceeds via reduction of the oxide by the reactant, which is then reoxidized by molecular oxygen to its original state in accordance with the Mars and van Krevelen redox mechanism.[1] In addition to oxidation reactions, transition metals play an important role in the activation of C−C and C−H bonds in alkanes and alkyl groups. Unraveling the mechanisms by which these reactions occur has been one of the most challenging projects in chemistry and continues to be an intensively studied subject. Although catalysis continues to have an enormous impact on technology, our ability to design catalysts that will lead to the facile formation of desired products with high selectivity and minimal environmental impact is quite rudimentary. Although the lack of knowledge about the basic mechanisms by which various catalysts function has impeded the ability to design new materials, there are encouraging prospects suggesting that ultimately this goal can be achieved.

Early transition metal oxides, and particularly vanadium-containing oxides, are important catalysts for many industrial applications and specifically for oxygen transfer reactions.[2−8] Many studies have been performed to gain insight into the mechanism for oxovanadium catalysis.[9−11] One of the most complicated of these systems is the oxidation of *n*-butane to maleic anhydride (MA) on the vanadyl pyrophosphate (VPO) surface.[12−14] This reaction involves the abstraction of eight hydrogen atoms (resulting in the formation of four water molecules) and the insertion of three oxygen atoms, which constitutes a 14-electron-transfer process.[15,16] The mechanism for this reaction has been debated extensively over the past decade due to its complexity and the lack of observed intermediate species during the steady-state production of MA. It was first proposed that the reaction followed an olefinic route. This mechanism involves the successive conversion of *n*-butane to butene and then to butadiene before insertion of the oxygen atoms to form furan and finally MA[16] (the intermediate species were proposed to be able to readily desorb from the surface). However, the basis for this mechanism was conceived using nonstandard conditions where traces of alkenes and furan intermediates have been observed when low oxygen and high *n*-butane concentrations were used over vanadium phosphorus oxide catalysts with average vanadium oxidation states of ∼4 or below.[16−18] Numerous studies have since followed and it is now believed that the oxidation of *n*-butane to MA follows an alkoxide route in which the reactant and subsequent intermediates do not leave the surface until completion of the reaction where upon the final product, MA, is released.[19]

Until recently, our understanding of heterogeneous catalysis and the mechanisms by which these processes take place has come predominantly from characterization of catalysts and reactions that occur at gas−solid or liquid−solid interfaces and in solutions. Gas-phase studies of clusters provide an alternative method from which to gain information that is applicable to reactant interactions with the surfaces of bulk materials. The

† Part of the special issue "Jack Beauchamp Festschrift".

10.1021/jp020559g CCC: $22.00
Published on Web 08/15/2002

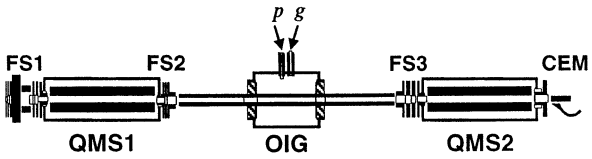

Figure 1. Schematic representation of the guided ion beam mass spectrometer, which is comprised of the first focusing stage (FS1), the first quadrupole (QMS1), the second focusing stage (FS2), the octopole ion guide (OIG), the third focusing stage (FS3), the second quadrupole (QMS2) and the dynode channel electron multiplier (CEM). The reactant gas enters the center of the cell through gas inlet g. The pressure is monitored through outlet p, which is perpendicular to the gas inlet (shown side-by-side for clarity).

intrinsic reactivity of the metal can thus be understood in the absence of solvent and aggregation effects. It is believed that these types of gas-phase studies will aid in unraveling the influences of such factors as cluster composition, stoichiometry, size, ligation, oxidation- and charge-states, ionization potentials, electron affinities, cluster temperature, as well as the electronic and geometrical structures of the clusters, all of which potentially influence catalytic behavior. Thereby, valuable information about possible reaction intermediates, reaction mechanisms, and the relationship between cluster structure and reactivity can be derived. By studying transition metal oxides in the gas-phase, the composition, stoichiometries, oxidation-, and charge-states can be precisely controlled to determine the effects that these factors have on catalytic behavior. This is difficult to achieve using conventional surface preparation and spectroscopic techniques in which the creation and identification of particular sites is difficult if not impossible. In many cases, these findings can substantially contribute to a greater understanding of the active sites of metal catalysts with reactant molecules for revealing elementary reactions that are important in their functioning. It is known that the reactivity of clusters in a given size regime may represent an accurate model of the bulk material.[20−22] Through the use of a versatile, quadrupole-based tandem mass spectrometer, findings from our laboratory have provided considerable new insight into the role that such factors have on catalytic active sites. In particular, we have found significant dependence of these factors for various mechanisms including oxidative dehydrogenation, oxygen-transfer, oxidation and cracking reactions.

Experimental Section

A guided ion beam tandem mass spectrometer was used for the current studies; the details for which have been reported previously.[23] The guided ion beam mass spectrometer (Figure 1) was used to study the low-pressure reactivities of cluster ions. Mass selected ions of well-defined kinetic energy are allowed to react with neutral molecules under single and multiple collision conditions. The reactions occur inside an octopole ion guide where the scattered products are trapped in the axial direction. Quadrupole mass filters are used for the selection and analysis of ionic species and detected by a channel electron multiplier (CEM).

The ions produced in the present work were formed in a laser vaporization (LAVA) source. This type of source creates copious amounts of ionic clusters with stoichiometries that can be varied by slightly changing the conditions under which they are produced. The second harmonic output (532 nm) of a Nd:YAG laser with a 20 Hz repetition rate at 220 mJ/pulse is used for these experiments. However, it is necessary to attenuate the light to achieve the approximately 5 to 26 mJ per pulse needed for optimal cluster production. The laser is focused to an approximate area of 0.5 mm^2 on the surface of a rotating, translating vanadium rod.

The experimental cycle begins with a pulse of helium carrier gas seeded with the reactant gas of choice (oxygen for these studies). The pulse is created by a solenoid valve (General Valve, Series 9) that is driven by a homemade pulsed valve driver with a fixed backing pressure of 6.6 atm. The cluster ions formed in the plasma reactions are carried by the diffusion of the carrier gas. After exiting the LAVA source, the ions are cooled through supersonic expansion and then transverse a 25 cm field free region in the source chamber before passing through a 3 mm diameter skimmer, which forms the molecular beam. The skimmer also acts to isolate the source chamber from the reaction chamber allowing differential pumping of these regions. Thereafter, the ions are focused and steered by the first focusing stage, which comprises a set of electrostatic ion lenses and deflectors, and then injected into the first quadrupole for mass selection. Both cationic and anionic species are formed in the LAVA source. The polarity of the dc potentials applied to both the electrostatic lenses and the rods of the rf devices determine which species are to be studied.

The focusing stages before and after the reaction cell (octopole ion guide) consist of extraction and injection lenses along with several other electrostatic lenses for collimating the beam prior to injection into the reaction cell or refocusing of the ionic species after extraction from the cell. The nominal ion energy for the reactions performed in the ion guide was maintained at ground potential for these studies. Under these conditions, the potential on the injection lens was kept at 30 V, while the extraction lens was maintained at ~200 V to ensure proper collection of products produced with small kinetic energies. Finally, the ions are extracted from the last quadrupole through a single tube lens and are strongly attracted to the 5000 V potential applied to the dynode of the CEM.

The octopole ion guide utilizes 3.57 mm diameter stainless steel rods, 40.6 cm long that are held on a 1.27 cm diameter circumference where the radius created by the inner surface of the rods is 5.18 mm. The stainless steel reaction cell consists of an 11.4 cm body with an inside diameter of 5 cm. To this body, two 1.5 cm long mounting tubes with inside diameters of 3.8 cm are welded to either side. Inside the mounting tubes, two 1 cm long ceramic disks support the rods of the octopole creating an inside diameter of 1.14 cm. This effectively creates 10.4 mm diameter openings at either end of the cell. Using a trapezoidal pressure falloff approximation,[24] the effective path length of the cell was determined to be 12.9 cm. This represents the length of the main cell body and the contribution of the mounting tubes where the pressure inside the main cell body is expected to fall off linearly to the background pressure at the openings of the mounting tubes. The neutral reactant gas is introduced into the center of the cell. The pressure inside the cell is measured through the center of the cell perpendicular to the gas inlet. The tubes that connect the gas cells to the capacitance manometers are about 20 cm long with ~3 mm inside diameters. This is relatively small compared to the mean free path of the gas. Therefore, the pressure must be corrected for thermal transpiration.[25] The gas cell temperature is estimated to be ~305 K for the octopole ion guide as found by other researchers using a chromel/alumel thermocouple with a similar instrument.[26] This is slightly elevated from ambient temperature due to rf power dissipation of the ion guides. The oscillator frequency is maintained at 2.8 MHz and is slightly adjustable using a high voltage variable capacitor. A high trapping

efficiency is accomplished by operating the octopole above a peak-to-peak rf voltage of 250 V.

A quadrupole mass filter is used for product mass determination, which provides unit mass resolution when properly operated. However, when collecting data for quantitative measurements, the resolution is set as low as possible while still maintaining adequate mass separation. The quadrupole could discriminate against strongly scattered or low energy products if the resolution is set too high. Although it is theoretically possible to operate the quadrupole at higher resolutions and apply mass discrimination corrections, the transmission of secondary ions is dependent on the reaction dynamics as well as mass. For these reasons, the quadrupole resolution is kept as low as possible and no corrections for mass discrimination are made. The ions are detected with a dynode channel electron multiplier (CEM) that is attached to the end of the last quadrupole. The polarity of the dynode determines the species that are detected. The detector is operated in the pulse counting mode and the raw output of the CEM is filtered and amplified by a 50 MHz preamplifier-discriminator pad (MIT, Model F-100T). The data are acquired through a TTL input by a multichannel scaler (MCS) card contained within a PC. The data can be analyzed using the MCS program or the format may be converted for analysis in other data software packages.

Results

The reactions of the clusters $V_3O_6^+$, $V_3O_7^+$, and $V_3O_8^+$ with 1,3-butadiene (C_4H_6) and selectively and fully deuterated 1,3-butadienes (1,1,4,4-d4-$C_4D_4H_2$ and C_4D_6) are studied to determine the products and possible reaction mechanisms. These studies are meant to complement previous investigations from our laboratory that examined the reactivity of vanadium oxide cluster cations with 1,3-butadiene and 1-butene in a quadrupole reaction cell.[27] The current studies utilized the octopole ion guide in which the pressure was varied between 0.05 and 0.40 mTorr. This represents the range of single to multiple collision conditions, with single collision conditions being obtained at pressures less than 0.08 Torr. Increasing the pressure resulted in the steady increase of reaction products, whereas no new products were observed to appear as reported previously.[27] All results reported herein are performed at thermal energies, that is, both the creation (LAVA ion source) and reaction (octopole rods and cell) of the clusters occur at ground potential, while the reactant gas is at ambient temperature (~305 K). The cluster $V_3O_6^+$ is found to be relatively unreactive with 1,3-butadiene under these conditions to form a single product, namely, molecular association to form $V_3O_6C_4H_6^+$ as seen in Figure 2a. Reaction products created by fast ions or other metastable species produced in the LAVA source are monitored while deflecting all ions and maintaining the same reactant gas pressure in the reaction cell. This background spectrum is then subtracted from the data collected for the mass selected ion over the same mass range. Our current experimental setup does not allow for the structural characterization of the reaction products and, therefore, distinction between addition or association channels is not possible, but we will refer to these species as association products for descriptive ease. The cluster $V_3O_7^+$ is more reactive with C_4H_6 as is evident from the spectrum shown in Figure 2b. A prominent channel for charge transfer to form $C_4H_6^+$ is observed, which is also observed for the deuterated species as well. Other products found for this reaction are loss of a single oxygen to form $V_3O_6^+$, oxidative dehydrogenation to form $V_3O_6C_4H_4^+$ and an association product $V_3O_7C_4H_6^+$, as

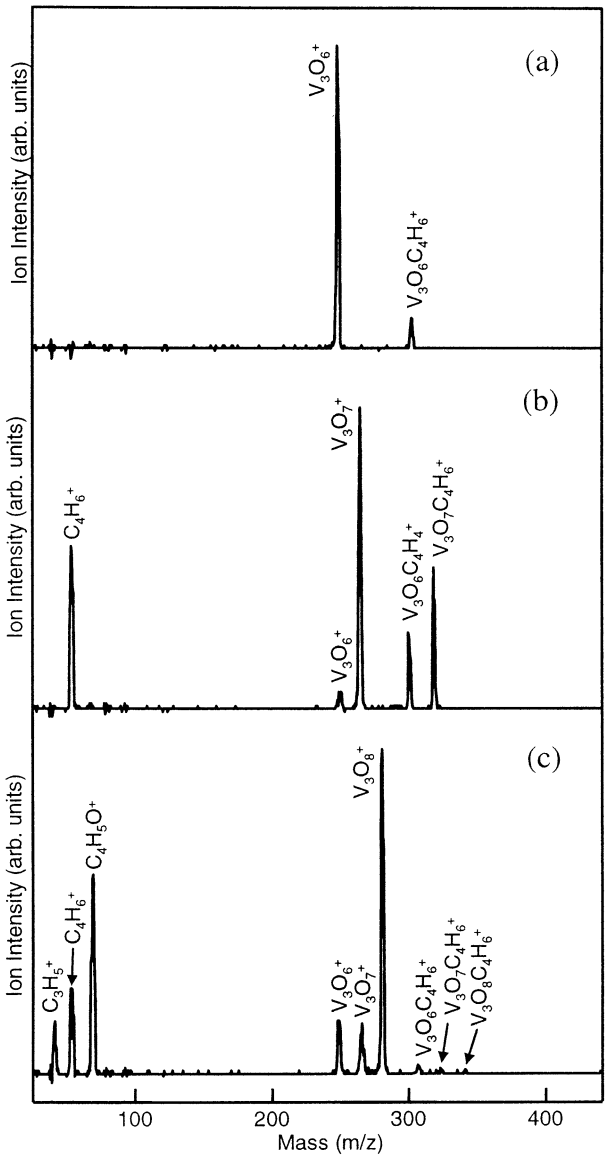

Figure 2. Spectra for the reactions of (a) $V_3O_6^+$, (b) $V_3O_7^+$, and (c) $V_3O_8^+$ with 0.29 mTorr of 1,3-butadiene. The background products caused by fast ions under the same conditions have been subtracted from each spectrum.

reported previously,[27] and confirmed with the fully deuterated hydrocarbon as summarized in Table 1. The oxidative dehydrogenation channel displays both of the products $V_3O_6C_4D_2H_2^+$ and $V_3O_6C_4D_3H^+$ for the selectively deuterated butadiene. The cluster $V_3O_8^+$ is found to be highly reactive with 1,3-butadiene forming the oxygen-loss products $V_3O_6^+$, $V_3O_7^+$, and the association products $V_3O_6C_4H_6^+$, $V_3O_7C_4H_6^+$ and $V_3O_8C_4H_6^+$. The charge-transfer channels forming $C_4H_6^+$ and the fragmentation product $C_3H_5^+$ are also observed. However, $C_4H_5O^+$ is found to dominate the reaction as seen in the spectrum in Figure 2c. These assignments are confirmed using C_4D_6. A summary of the reaction channels for these clusters with 1,3-butadiene is given in Table 1.

The anions do not demonstrate the same reactivity observed for the cations. In fact, the clusters $VO_{2,3}^-$, $V_2O_{4,5}^-$, $V_3O_{6-8}^-$, and $V_4O_{10}^-$ do not react with either 1,3-butadiene or 1-butene while clusters of higher oxygen content, $V_2O_6^-$, $V_3O_9^-$, and $V_4O_{11}^-$ display a minor reaction channel for the loss of a single oxygen atom, presumably as oxidation of the hydrocarbon

TABLE 1: Reaction of Vanadium Oxide Cluster Cations $V_3O_6^+$, $V_3O_7^+$, and $V_3O_8^+$ with the Isotopes of 1,3-butadiene, Namely, C_4H_6, C_4D_6, and 1,1,4,4-d4-$C_4D_4H_2$ at near Thermal Energies and a Reactant Pressure of 0.15 MTor

selected cluster	reactant gas (C_4H_6)	1,3-butadiene (C_4H_6)	(1,1,4,4-d4-$C_4D_4H_2$)
$V_3O_6^+$	(C_4D_6)	$V_3O_6C_4D_6^+$	$V_3O_6C_4D_6H_2^+$
$V_3O_7^+$	$C_4H_6^+$	$C_4D_6^+$	$C_4D_4H_2^+$
	$V_3O_6^+$	$V_3O_6^+$	$V_3O_6^+$
	$V_3O_6C_4H_4^+$	$V_3O_6C_4D_4^+$	$V_3O_6C_4D_2H_2^+$
	$V_3O_7C_4H_6^+$	$V_3O_7C_4D_6^+$	$V_3O_6C_4D_3H^+$
			$V_3O_7C_4D_4H_2^+$
$V_3O_8^+$	$C_3H_5^+$	$C_3D_5^+$	
	$C_4H_6^+$	$C_4D_6^+$	
	$C_4H_5O^+$	$C_4D_5O^+$	
	$V_3O_6^+$	$V_3O_6^+$	
	$V_3O_7^+$	$V_3O_7^+$	
	$V_3O_6C_4H_6^+$	$V_3O_6C_4D_6^+$	
	$V_3O_7C_4H_6^+$	$V_3O_7C_4D_6^+$	
	$V_3O_8C_4H_6^+$	$V_3O_8C_4D_6^+$	

resulting in the cluster $V_xO_{y-1}^-$. We believe this to be oxidation of the hydrocarbon and not a collision-induced dissociation product, due to the fact that loss of a single oxygen atom from these species is an activated process that does not occur at thermal energies.[23] The lack of reactivity of the anionic species is not surprising, as hydrocarbons (C_nH_m) do not readily ligate with anions.[28]

The reactions of $V_3O_7^+$ with the isomers of butene (1-butene, *cis*-2-butene, and *trans*-2-butene) are studied to further understand the mechanism by which hydrocarbons react with vanadium oxide cluster ions. The reactions of this cluster with the butenes are slightly different than those with 1,3-butadiene. The charge-transfer products $C_4H_8^+$ and with hydrogen atom abstraction to form $C_4H_7^+$ are observed for all three isomers. The cis- and trans- isomers react similarly to produce nearly equal quantities of both $C_4H_8^+$ and $C_4H_7^+$ at a reactant pressure of 0.20 mTorr in the collision cell as seen in Figure 3 for *cis*-2-butene. Although not shown for 1-butene, the $C_4H_7^+$ product is found to be favored by about 4 to 1 compared to $C_4H_8^+$ at 0.20 mTorr. The butene isomers, however, do produce some of the same types of products that are observed for the reactions of 1,3-butadiene, namely, $V_3O_6^+$, oxidative dehydrogenation ($V_3O_6C_4H_6^+$), molecular association ($V_3O_7C_4H_8^+$) and a channel for C2−C3 cracking of the alkene forming $V_3O_7C_2H_4^+$ is observed, as reported previously for 1-butene.[27] In addition, an intense channel representing dehydrogenation of the alkene to form $V_3O_7H_2^+$ is observed. This product was not reported previously due to the inadequate resolution of the previous instrument. The branching ratios for the reaction of $V_3O_7^+$ with 1-butene, *cis*-2-butene, and *trans*-2-butene can be seen in Figures 4 through 6, respectively.

Discussion

The condensed phase VO_4 unit has attracted much attention due to its important role in oxovanadium catalysis.[29] This species is not equivalent to either the neutral or ionic gas-phase clusters in the size regime currently under study as three of the oxygen in this condensed phase species are shared with other vanadium centers, but the fourth oxygen forms a vanadyl (−V═O) group. Importantly, this oxovanadium species contains the vanadium center in the +5 oxidation state, which is thought by many researchers to be the necessary state for oxygen transfer to occur.[15] Another difference between that of bulk vanadium oxide and the gas-phase clusters studied is the size difference of the two systems; the clusters examined here are small and coordinatively unsaturated. On the other hand, it is thought that they

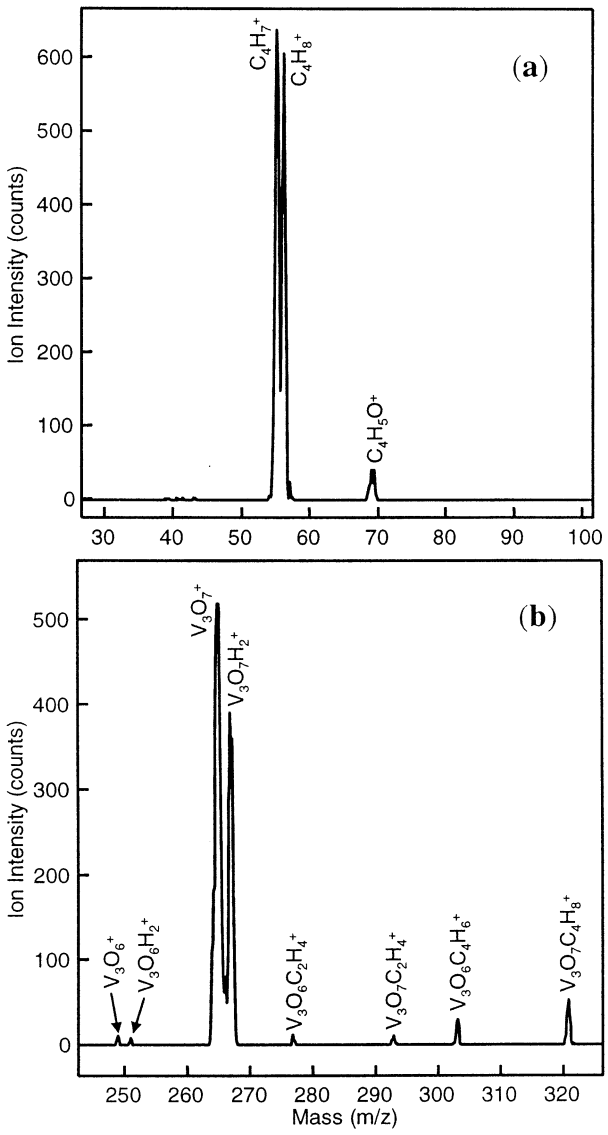

Figure 3. Spectra for the reaction of $V_3O_7^+$ with 0.20 mTorr of *cis*-2-butene. The products for the (a) non-vanadium containing species are shown in the upper spectrum and those for the (b) vanadium containing species are shown in the lower spectrum.

may be representative of defect sites on the bulk surface. Indeed, many of the reaction channels found in these gas-phase studies appear to be consistent with those that occur in the condensed phase. Therefore, we shall discuss the results in comparison with the condensed phase reactions of vanadium oxide catalysts with the intent that this information will aid in further understanding the mechanisms involved in oxygen transfer processes.

Formation of the intermediates of butene and butadiene in the transformation of *n*-butane to maleic anhydride (MA) is unlikely, as these products are not observed in this steady-state industrial process. There is, however, strong experimental evidence that the formation of MA occurs in successive steps on the VPO surface to form the oxygenated intermediates that may diffuse along the surface, but not necessarily released into the gas-phase.[19] The greatest barrier of activation for the oxidation of *n*-butane is found to be the first oxidative dehydrogenation (ODH) to form H_2O and the dehydrogenated product.[30,31] As a result, the reaction conditions needed to overcome this first step results in the total conversion to MA

and the major byproducts H_2O, CO, and CO_2 under aerobic conditions. Partial dehydrogenation can be achieved, however, under conditions that separate the reduction and oxidation steps of the process. For example, using a two-zone fluidized-bed reactor, the selectivity and conversion *n*-butane to 1,3-butadiene by ODH over a V/MgO catalyst can be controlled.[32] Our gas-phase reactions may be considered as reactions that occur under anaerobic conditions because there is no gas-phase (or lattice) oxygen to replenish the loss of "surface" oxygen. Therefore, we are able to look at one step of the reaction at a time.

The role of the oxidation state of the vanadium in the active catalyst has been of much debate over the years. However, oxygen transfer is generally believed to occur in the presence of mixed valance sites containing the V^{4+}—V^{5+} pair in close proximity to one another or at isolated V^{5+} sites.[33−37] We have studied the role of vanadium oxidation state on hydrocarbon reactions in the past and have shown a strong dependence on the V^{5+} center for oxygen transfer or oxidative dehydrogenation of the hydrocarbon.[27] These results demonstrated that clusters containing vanadium centers with oxidation states below +5, i.e., $V_3O_6^+$ that has a +4.67 overall oxidation state, did not display channels for oxygen transfer, whereas clusters with +5 or higher oxidation states, i.e., $V_3O_7^+$ (+5 average oxidation state) and $V_3O_8^+$ (greater than +5 average oxidation state and/or possible activated oxygen species) do display oxygen transfer channels. The current studies contribute to a further understanding of these gas-phase reactions.

The reaction of the cluster $V_3O_7^+$ with the alkenes displays a channel for ODH where two hydrogen atoms are abstracted from the hydrocarbon, releasing H_2O. The dehydrogenated hydrocarbon remains attached to the cluster. This is shown in eqs 1 and 2 for 1,3-butadiene and the isomers of butene, respectively

$$V_3O_7^+ + C_4H_6 \rightarrow V_3O_6C_4H_4^+ + H_2O \quad (1)$$

$$V_3O_7^+ + C_4H_8 \rightarrow V_3O_6C_4H_6^+ + H_2O \quad (2)$$

This indicates that the abstraction of the 2 hydrogen atoms occurs in the vicinity of a single oxygen site. There are two possible mechanisms for this reaction. First, the alkene may associate to the cluster across the carbon double bond, whereupon abstraction of the hydrogen may occur from either of the carbons across this bond with rearrangement to a favorable state. A second possible mechanism is the formation of a cyclic structure with the C1 and C4 carbons associated to the cluster. In this scenario, the abstraction of the hydrogen should occur at these terminal carbons. In an attempt to further understand the mechanism behind the ODH, we examined the reaction of the selectively deuterated 1,1,4,4-d4−1,3-butadiene. This reaction, however, demonstrates ODH channels that produce both D_2O and HDO. Therefore, it is still not clear as to which of these mechanisms, if not both, are operative.

However, this reaction does show us that a vanadyl oxygen in the +5 oxidation state is required for this reaction. ODH must occur at a vanadyl site and not a bridging site (−V−O−V−) or fragmentation of the cluster would have been observed. Mechanisms that involve the abstraction of bridging oxygen atoms of the cluster have resulted in the fragmentation of the $V_xO_y^+$ clusters. For example, the reactions of vanadium oxide cluster cations with carbon tetrachloride (CCl_4) have displayed fragmentation channels leading to the loss of vanadium from the cluster.[38] These reactions were consistent with the mechanisms found for the degradation of CCl_4 on bulk phase vanadium oxide catalysts where the loss of the vanadium surface in the form of $VOCl_2$ and volatile $VOCl_3$ was experimentally observed.[39] This is not to say that oxidation of the hydrocarbons does not use bridging oxygen atoms in the condensed phase lattice, but if so, then they must occur at higher energies than those which are found for the present gas-phase experiments.

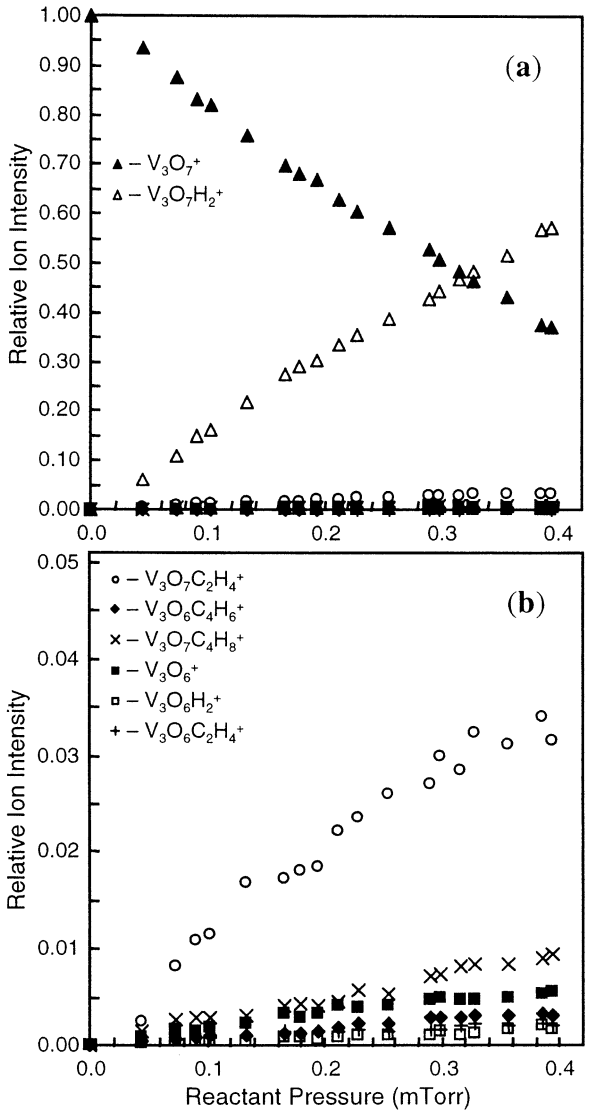

Figure 4. Partial branching ratios of the vanadium-containing products for the reaction of (a) $V_3O_7^+$ with 1-butene and (b) the expanded view of the minor products. Dehydrogenation to form $V_3O_7H_2^+$ is the dominant reaction channel. Cracking of the C2−C3 bond is more prevalent then that of oxidative dehydrogenation.

The presence of gas-phase oxygen has been considered detrimental to the selectivity of transition metal oxide catalysts. The electrophilic surface species of adsorbed oxygen such as O^- and O_2^- have long been believed to be very active in the complete oxidation of hydrocarbons.[40] This has led to the design of various reactors that attempt to separate the catalytic process resulting in the reduction of the catalyst by the hydrocarbon and then reoxidation of the catalyst by oxygen to minimize the presence of gas-phase oxygen in the reaction atmosphere.[41−43] However, complete separation of the redox cycle is not favorable due to the intrinsic instability of catalytic behavior associated with anaerobic operation of fixed bed catalysts. Therefore, low concentrations of gas-phase oxygen are required to improve selectivity of the catalyst.[44,45]

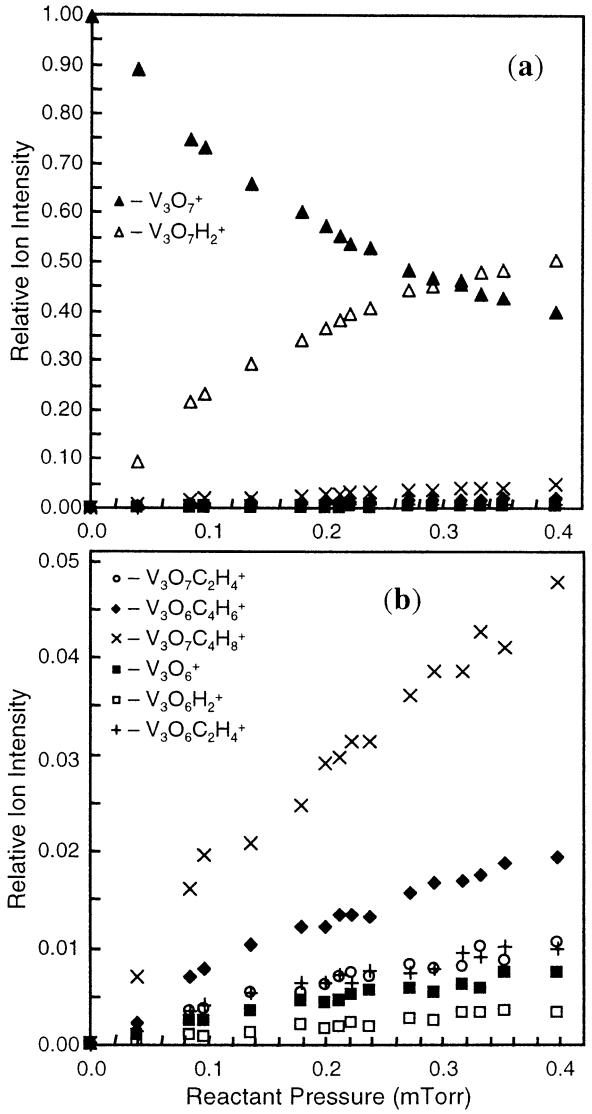

Figure 5. Partial branching ratios of the vanadium-containing products for the reaction of (a) $V_3O_7^+$ with *cis*-2-butene and (b) the expanded view of the minor products. Dehydrogenation to form $V_3O_7H_2^+$ is the dominant reaction channel. Oxidative dehydrogenation is more prevalent then that of cracking of the C2−C3 bond.

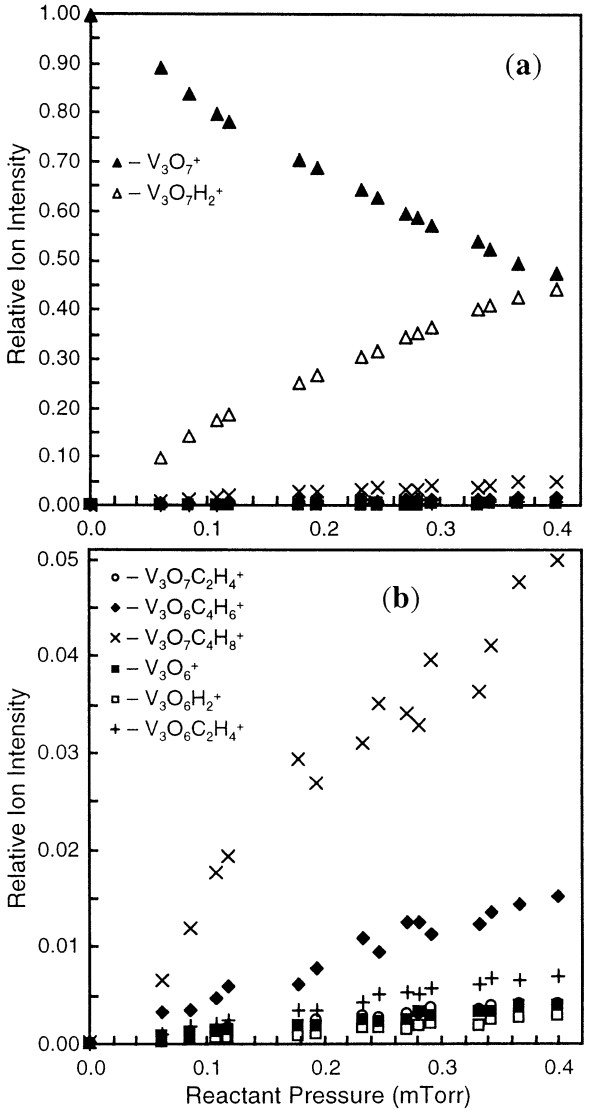

Figure 6. Partial branching ratios of the vanadium-containing products for the reaction of (a) $V_3O_7^+$ with *trans*-2-butene and (b) the expanded view of the minor products. Dehydrogenation to form $V_3O_7H_2^+$ is the dominant reaction channel. Oxidative dehydrogenation is more prevalent then that of cracking of the C2−C3 bond.

Studies using isotopic labeling of gas-phase oxygen, $^{18}O_2$, to determine the effect of gas-phase oxygen on the conversion of *n*-butane to MA and other products have been performed by a number of researchers.[46−48] These studies tend to suggest that MA, H_2O, CO, and CO_2 production are not influenced by the presence of gas-phase oxygen. Only after a short time do the labeled products show up, indicating that oxygen insertion of all of these species occurs with lattice oxygen and not activated oxygen species. The labeled oxygen only becomes involved in the reaction after adsorption into the lattice. However, these studies do not role out the possibility that active oxygen sites were already present on the surface before the introduction of $^{18}O_2$. Both the present and past[27] findings indicate that clusters with activated oxygen,[23] such as, $V_3O_8^+$, are highly reactive and nonselective with 1,3-butadiene displaying various channels for oxygen transfer and, also, a fragmentation channel forming $C_3H_5^+$. In fact, the most active channel is for the charge-transfer product $C_4H_5O^+$. This is indicative of a highly reactive oxygen species on these clusters.

Recent studies on the reactions of the isomers of butene over VMgO catalysts demonstrated little difference for the ODH of these isomers.[49] The authors of this work report a slight preference for the selectivity to butadiene of 65% for the cis- and *trans*-2-butenes compared to the 64% for 1-butene. On the basis of the reaction rates determined from their study, the apparent activation energies for ODH of 1-butene is 85 kJ/mol compared to 82 kJ/mol for the 2-butenes. Our gas-phase studies display similar results for the ODH of the isomers of butene. This can be seen in the branching ratios in Figures 4-6 for the ODH products $V_3O_7H_2^+$ and $V_3O_6C_4H_6^+$, which are similar for all three isomers. The neutral products released in these reactions are expected to be 1,3-butadiene and water, respectively

$$V_3O_7^+ + C_4H_8 \rightarrow V_3O_7H_2^+ + C_4H_6 \quad (3)$$

$$V_3O_7^+ + C_4H_8 \rightarrow V_3O_6C_4H_6^+ + H_2O \quad (4)$$

Another reaction channel is that of cracking of the alkene to form the product $V_3O_7C_2H_4+$. The 1-butene displays a slightly higher selectivity toward this channel as seen in the expanded views of the branching ratios of these reactions. This could

explain the slightly higher selectivity of the 2-butenes for the production of 1,3-butadiene on the bulk phase catalyst.[49]

Conclusions

These results demonstrate the importance of the vanadyl group in the +5 oxidation state for oxygen transfer reactions in the gas-phase chemistry of vanadium oxide cluster ions. It is still unclear as to the exact mechanism responsible for ODH of 1,3-butadiene on these clusters, as indicated by the loss of both neutral DHO and D_2O products from the selectively deuterated 1,1,4,4-d4−1,3-butadiene. The release of neutral water from this reaction is indicative of both H abstractions occurring at the same vanadium site and possibly by the same oxygen atom. Lack of fragmentation of the cluster demonstrates that the ODH process occurs at a vanadyl site and not a bridging oxygen site. Again, these studies confirm the presence of active oxygen species on clusters of high oxygen content, i.e., $V_3O_8^+$, which demonstrates a variety of pathways for oxygen transfer and even cracking of the alkene. Our results suggest that ODH of *cis*- or *trans*-2-butene is slightly favored in comparison to that of 1-butene. Cracking of both 1- and 2-butenes is observed, although cracking is observed to occur slightly more readily with 1-butene. These gas-phase cluster studies clearly indicate a number of similarities with condensed phase reactions. It is believed that further comparison between these different phases of chemistry will lead to a better understanding of both.

Acknowledgment. Financial support by the National Science Foundation, Grant No. CHE-99-06341 is gratefully acknowledged.

References and Notes

(1) Mars, P.; van Krevelen, D. W. *Chem. Eng. Sci. (Spec. Suppl.)* **1954**, *3*, 41.
(2) Anderson, J. R.; Boudart, M. *Catalysis: Science and Technology*; Springer-Verlag: Berlin, 1984.
(3) Bond, G. C. *J. Catal.* **1989**, *116*, 531.
(4) Anderson, A.; Lundin, S. T. *J. Catal.* **1979**, *58*, 383.
(5) Hirao, T. *Chem. Rev.* **1997**, *97*, 2707.
(6) Ramírez, R.; Casal, B.; Utrera, L.; Ruiz-Hitzky, E. *J. Phys. Chem.* **1990**, *94*, 8960.
(7) Legrouri, A.; Baird, T.; Fryer, J. R. *J. Catal.* **1993**, *140*, 173.
(8) Grzybowska-Swierkosz, B., Trifiro, F., Vedrine, J. C. ,Eds.; Vanadia Catalysts for Selective Oxidation of Hydrocarbons and Their Derivatives. *J. Appl. Catal.* **1997**, *157*, 1−425.
(9) (a) Oyama, S. T. *Catal. Today* **1992**, *15*, 179. (b) Oyama, S. T. *J. Solid State Chem.* **1992**, *96*, 442.
(10) Deo, G.; Wachs, I. E. *J. Catal.* **1994**, *146*, 323.
(11) Chen, S. Y.; Willcox, D. *Ind. Eng. Chem. Res.* **1993**, *32*, 584.
(12) Hodnett, B. K. *Catal. Rev. Sci. Eng.* **1985**, *27*, 373.
(13) Gai, P. L.; Kourtakis, K. *Science* **1995**, *267*, 661.
(14) Cavani, F.; Trifiro, F. *Catalysis* **1994**, *11*, 246.
(15) Centi, G. *Catal. Today* **1993**, *16*, 5.
(16) Centi, G.; Trifiro, F.; Ebner, J. R.; Franchetti, V. M. *Chem. Rev.* **1988**, *88*, 55−80.
(17) Kubias, B.; Rodemerck, U.; Zanthoff, H. W.; Meisel, M. *Catal. Today* **1996**, *32*, 243.
(18) Rodemerck, U.; Kubias, B.; Zanthoff, H. W.; Wolf, G. U.; Baerns, M. *Appl. Catal. A-Gen.* **1997**, *153*, 217.
(19) Aguero, A.; Sneeden, R. P.; Volta, J. C. In. Heterogeneous Catalysis and Fine Chemicals. *Studies in Surface Science and Catalysis*; Guisnet, M., Ed.; Vol. 41, Elsevier: Amsterdam, 1988; p 353.
(20) (a) Somorjai, G. A. *Chem. Rev.* **1996**, *96*, 1223. (b) Somorjai, G. A. *Introduction to Surface Chemistry and Catalysis*; Wiley: New York, 1994; pp 402−409.
(21) Rhodin, T. N., Ertl, G., Eds.; *The Nature of the Surface Chemical Bond*; North-Holland: New York, 1979; Chapter 2.
(22) Moskovits, M. *J. Mol. Catal.* **1993**, *82*, 195.
(23) Bell, R. C.; Zemski, K. A.; Justes D. R.; Castleman, Jr., A. W. *J. Chem. Phys.* **2001**, *114*, 798.
(24) (a) Rosion, S.; Rabi, I. I. *Phys. Rev.* **1935**, *48*, 373. (b) Amdur, I.; Jordon, J. E. *Adv. Chem. Phys.* **1966**, *10*, 29.
(25) (a) Maxwell, J. C. *Philos. Trans. R. Soc. London* **1879**, *170*, 231. (b) Loriot, G.; Moran, T. *Rev. Sci. Instrum.* **1975**, *46*, 140.
(26) Ervin, K. M.; Armentrout, P. B. *J. Chem. Phys.* **1985**, *83*, 166.
(27) Bell, R. C.; Zemski, K. A.; Kerns, K. P.; Deng, H. T.; Castleman, Jr., A. W. *J. Phys. Chem. A* **1998**, *102*, 1733.
(28) (a) Berg, C.; Beyer, M.; Achatz, U.; Joos, S.; Niedner-Schatteburg, G.; Bondybey, V. E. *J. Chem. Phys.*, **1998**, *108*, 5398. (b) Cox, D. M.; Brickman, R.; Creegan, K.; Kaldor, A. *Phys. D*, **1991**, *19*, 353 (c) Zemski, K. A.; Justes, D. R.; Bell, R. C.; Castleman, Jr., A. W. *J. Phys. Chem. A* **2001**, *105*, 4410.
(29) Tran, K.; Hanning-Lee, M. A.; Biswas, A.; Stiegman, A. E.; Scott, G. W.; *J. Am. Chem. Soc.* **1995**, *117*, 2618.
(30) Centi, G.; Fornasari, G.; Trifirò, F. *Ind. Eng. Chem. Prod. Res. Dev.* **1985**, *24*, 32.
(31) Buchanan, J. S.; Sundaresan, S. *Appl. Catal.* **1986**, *26*, 211.
(32) Soler, J.; López Nieto, J. M.; Herguido, J.; Menéndez, M.; Santamaría, J. *Ind. Eng. Chem. Res.* **1999**, *38*, 90.
(33) (a) Zang-Lin, Y.; Forissier, M.; Sneeden, R. P.; Védrine, J. C.; Volta, J. C.; *J. Catal.* **1994**, *145*, 256. (b) Zang-Lin, Y.; Forissier, M.; Védrine, J. C.; Volta, J. C. *J. Catal.* **1994**, *145*, 267.
(34) Robert, V.; Borshch, S. A.; Bigot, B. *J. Mol. Catal. A* **1997**, *119*, 327.
(35) Sananes-Schulz, M. T.; Tuel, A.; Hutchings, G. J.; Volta, J. C.; *J. Catal.* **1997**, *166*, 388.
(36) Wang, D.; Kung, H. H.; Barteau, M. A. *Appl. Catal. A* **2000**, *201*, 203.
(37) Delichère, P.; Béré, K. E.; Abon, M.; *Appl. Catal. A* **1998**, *172*, 295.
(38) Bell, R. C.; Zemski, K. A.; Castleman, Jr., A. W. *J. Phys. Chem. A* **1999**, *103*, 1585.
(39) (a) Mink, G.; Bertóti, I.; Battistoni, C.; Székely, T. *React. Kinet. Catal. Lett.* **1985**, *27*, 39. (b) Ebitani, K.; Hirano, Y.; Kim, J.-H.; Morikawa, A. *React. Kinet. Catal. Lett.* **1993**, *51*, 351.
(40) Bielanski, A.; Haber, J. *Catal. Rev.-Sci. Eng.* **1979**, *19*, 1.
(41) Callahan, J. L.; Grasselli, R. K.; Milberger, E. C.; Strecker, H. A. *Ind. Eng. Chem. Prod. Res. Dev.* **1970**, *9*, 134.
(42) Jones, C. A.; Leonard, J. J.; Sofranko, J. A. *Energy Fuels* **1987**, *1*, 12.
(43) Contractor, R. M.; Garnett, D. I.; Horowitz, H. S.; Bergna, H. E.; Patience, G. S.; Schwartz, J. T.; Sisler, G. M. *Stud. Surf. Sci. Catal.* **1994**, *82*, 233.
(44) Coronas, J.; Menéndez, M.; Santamaría, J. *Chem. Eng. Sci.* **1994**, *49*, 2015.
(45) Coronas, J.; Menéndez, M.; Santamaría, J. *Chem. Eng. Sci.* **1994**, *49*, 4749.
(46) Kruchinin, Y. A.; Mishchenko, Y. A.; Nechiporuk, P. P.; Gelbshtein, A. I. *Kinet. Catal.* **1984**, *25*, 328.
(47) Pepera, M. A.; Callahan, J. L.; Desmond, M. J.; Milberger, E. C.; Blum, R. P.; Bremer, M. J. *J. Am. Chem. Soc.* **1985**, *107*, 4883.
(48) Abon, M.; Béré, K. E.; Delichère, P. *Catal. Today* **1997**, *33*, 15.
(49) Lemonidou, A. A. *Appl. Catal. A* **2001**, *216*, 277.